A Preliminary Study on the Self-Orgnization Process of Multi-Vortex *

ZHOU Jialing[1†](周嘉陵), MA Jingxian[2](马镜娴), CHEN Lianshou[3](陈联寿), and LUO Zhexian[2](罗哲贤)

1 *Jiangsu Meteorological Observatory, Nanjing* 210008

2 *Nanjing University of Information Science & Technology, Nanjing* 210044

3 *Chinese Academy of Meteorological Sciences, Beijing* 100081

(Received January 4, 2007)

ABSTRACT

In this paper, the self-organization process of the initially scattered 12 meso-β and -γ scale vortices evolving into a synoptic-scale typhoon-like vortex in the context of advection dynamics is numerically explored with an f-plane 2-D quasi-geostrophic vorticity equation model. The results show that the self-organization process was a step-by-step merging course, namely the two adjacent vortices first merged, then formed a tri-vortex flow pattern, and finally evolved into a resultant vortex of meso-α scale. Thus it can be seen as an interaction of binary vortices self-organization. Each initial vortex or vorticity lump confronted two ways out: it merged with an adjacent vortex, and thus became a source of the inner region vorticity of the new formed vortex; or it was stretched by the circulation of an adjacent vortex, and then became the vorticity source of the spiral band of new vortex. Similarly, each new formed vortex also confronted the two ways out, until the multi-vortex self-organized into a single vortex of lager scale. The representation precision of the initial vortex structure directly affected the speeds of the mutual rotation and merging of the resultant vortex. Therefore, it is important to provide an accurate description of initial vortex profiles. Finally, a property of the numerical solution of the self-organization for the 2-D quasi-geostrophic flow is that the total kinetic energy decays slowly, the total enstrophy decreases rapidly, and the circulation of the largest scale vortex grows quickly.

Key words: vortex, vortices merging, self-organization, 2-D quasi-geostrophic flow

1. Introduction

The latest research indicates that the self-organization process can be classified into two types with the preliminary exploration on non-axisymmetric binary vortices self-organization dynamics (Shen et al., 2006). The final vorticity piled up in the inner-region by the self-organization of original Vortices A and B, such as the merging process of the 9th and 10th typhoons of 1970. The other way for the main source of the final vorticity gathered in the inner-region is the circulation of initial Vortex A, while the outer-region spiral band is from that of Vortex B such as the formation of Typhoon Oliver.

In the real atmosphere, the observational facts of vortex self-organization process are not only limited over the West Pacific Ocean, but also on the Tibetan Plateau. There were a group of convection cells over the plateau on 9 August 1995 and they finally organized into a meso-α convective system (see Fig.3 in Ma et al., 1997), which were analyzed from the enhanced infrared satellite cloud picture. It is worthy of discussing further the possible physical course for the meso-α convective system formation.

According to Chen and Yau (2001), cloud cluster resembles to vortex. Therefore, self-organization problem of 12 meso-β and -γ scale cloud clusters identified from Fig.3a in the paper of Ma et al. (1997) can be considered as vortices. In this paper, preliminary numerical study is carried out to explore the dynamic mechanism of the self-organization process on the basis of binary-vortex self-organization research.

2. Model and experiment design

The quasi-geostrophic barotropic vorticity equation without forcing and dissipation used f-plane

*Supported by the Key Project of National Natural Science Foundation of China under Grant No. 40333028.

†Corresponding author: jsmodel@gmail.com.

assumption is adopted:

$$\frac{\partial}{\partial t}\nabla^2\psi + J(\psi, \nabla^2\psi) = 0, \tag{1}$$

where ψ is geostrophic stream function and J is Jacobian functor.

Equation (1) is converted into a non-dimensional equation by using characteristic horizontal scale L=500 km and characteristic velocity V=10 m s^{-1}.

The initial vorticity field, referred as $\xi(x, y, 0)$, is given by the following expression:

$$\xi(x, y, 0) = \sum_{i=1}^{12} \xi_i(x, y, 0), \tag{2}$$

where $\xi = \nabla^2\psi$, denoted the relative vorticity of 12 initial vortices, which are given by the following formula:

$$\xi_i(x, y, 0) = \begin{cases} \xi_0 \sin(\frac{x-x_{i1}}{x_{i3}-x_{i1}}\pi)\sin(\frac{y-y_{i1}}{y_{i3}-y_{i1}}\pi) \\ \qquad (x_{i3} \geqslant x \geqslant x_{i1}, y_{i3} \geqslant y \geqslant y_{i1}) \\ 0 \quad \text{the other areas,} \end{cases} \tag{3}$$

where (x_{i2}, y_{i2}) are the center coordinates of the initial vortices, and $x_{i2} = (x_{i3} - x_{i1})/2, y_{i2} = (y_{i3} - y_{i1})/2$. In this paper, we set $x_{i3} - x_{i1} = y_{i3} - y_{i1}$, which delineates a circular symmetric vortex.

For the f-plane assumption, there is no systemic shift for the initial vortices. Thus we set $\frac{\partial\psi}{\partial t} = 0$ on the south and north boundaries. However, on the east and west boundaries, a cyclic boundary condition is used.

Three experiments, whose integration time is 72 h, are performed with $\xi_0 = 20.0$ (non-dimensional quantity).

In Experiment A, computational domain is a square of 1000 km×1000 km with 251×251 grid points in total, I=1, 2,..., 251, increasing eastwards; J=1, 2,..., 251, increasing northwards. The grid distance is 4 km, and the time step Δt is 30 s. In the initial field, there are 12 meso-β and -γ scale quasi-circular vortices, with their center coordinates: (140, 130), (71, 81), (186, 118), (172, 94), (156, 84), (149, 108), (139, 99), (183, 159), (168, 170), (153, 182), (133, 176), and (93, 161), respectively. The 12 vortex radii r_i are 50, 32, 32, 24, 32, 16, 20, 40, 32, 40, 36, and 32 km. The values of $(I_{i3}, I_{i1}, J_{i3}, J_{i1})$ are obtained by calculating with the vortex center coordinates (I_{i2}, J_{i2}) and its radii r_i. Figure 1a shows the initial relative vorticity field.

In Experiment B, the computational domain is expanded 200 km outward along the four boundaries compared with the domain of Experiment A. The effects of computational domain size or the grid point numbers on the vortex self-organization process can be seen through the comparison of the results of Experiments A and B.

In Experiment C, computational domain is a square of 1000 km×1000 km with 501×501 grid points in total, I=1, 2,..., 501, increasing eastwards; J=1, 2,..., 501, increasing northwards. The grid distance is 2 km, and the time step is 30 s. Initially, there are 12 meso-β and -γ scale quasi-circular vortices, with their center coordinates: (279, 259), (141, 161), (371, 235), (344, 188), (311, 168), (299, 216), (277, 198), (366, 319), (336, 339), (306, 364), (266, 351), and (186, 321), respectively, and their radii are the same as those of Experiments A and B.

To investigate the effects of initial vortex structure on the self-organization process, Experiments A and C were designed with different horizontal grid-distances. In the initial vorticity fields, the largest vortex radius was 50 km, corresponding vortex profile given by 13 (or 26) grid points in Experiment A (or Experiment C), and the smallest radius was 16 km with its profile given by 5 (or 9) grid points.

3. Computational results

3.1 *Interactions of two vortices under the condition of* 12 *vortices co-existing environment*

Figure 1 shows the temporal variations of the relative vorticity field in Experiment A with a interval of half an hour. When t=0, Vortex-a was located next to the point O of the computational domain center and in its southeast was a small one referred as Vortex-b (Fig.1b).

In the period from t=0 to 90 min, Vortex-b circulation elongated (Figs.1b-d). Two and half an hours later, it has elongated, narrowed, and became a spiral

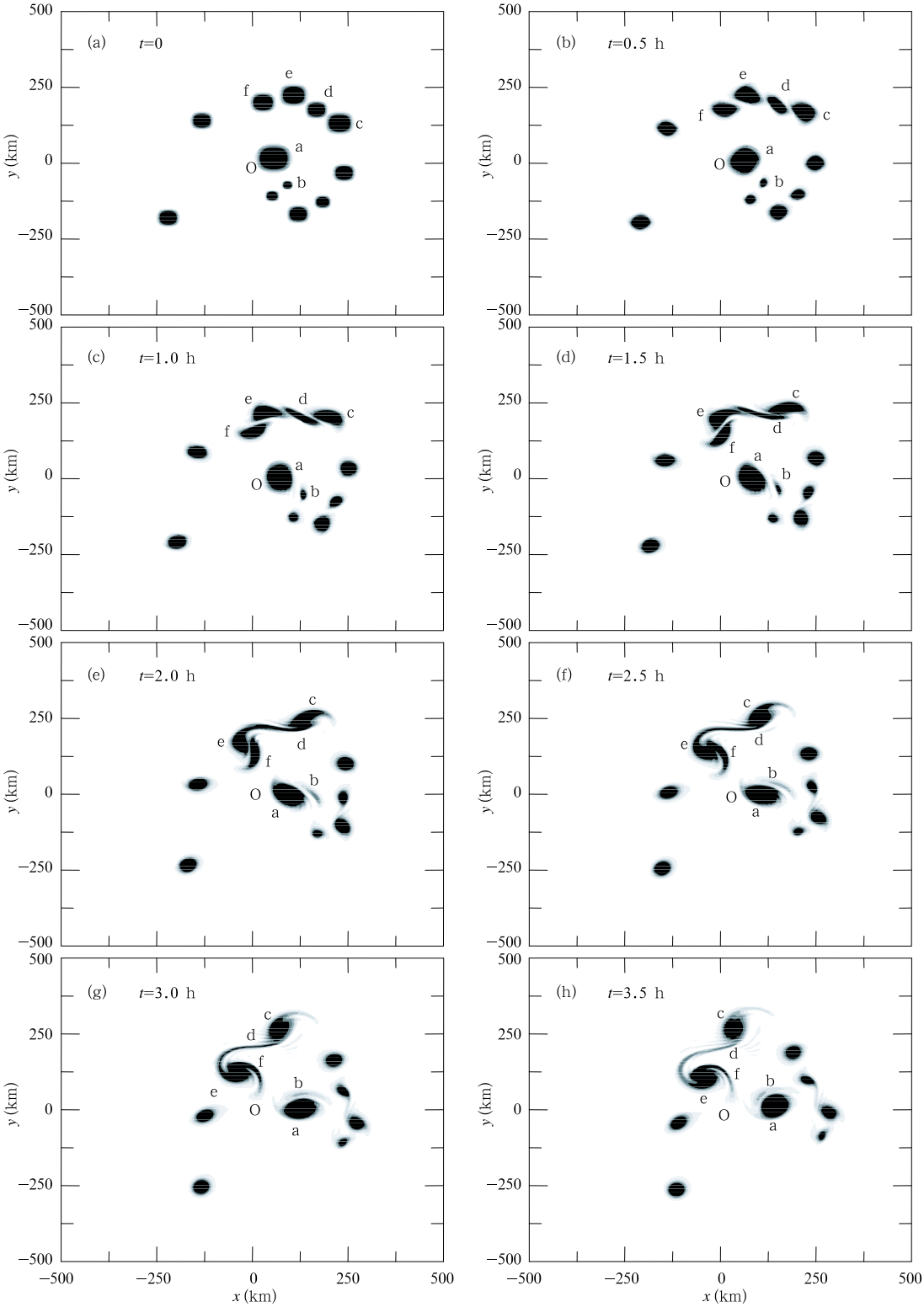

Fig.1. Temporal evolution of the relative vorticity field in Experiment A in the period of 0-3.5 h. (a) t=0, (b) t=0.5 h, (c) t=1.0 h, (d) t=1.5 h, (e) t=2.0 h, (f) t=2.5 h, (g) t=3.0 h, and (h) t=3.5 h; the boundary lines between different grayscale levels denote successively the relative vorticity of 1.0, 3.0, 5.0, 7.0, and 9.0.

vorticity band outward of the Vortex-a circulation. Synchronously, the outside vorticity wing gradually came into being by the part of vorticity of Vortex-a transferred outward (Figs.1e-h). This is the way how the smaller scale vortex absorbed by the larger one.

At initial time t=0 in Experiment A, besides Vortex-a and -b, there were Vortex-c and -d, which were located to the northeast of the point O (Fig.1a). At t=90 min, the Vortex-d circulation elongated to a vorticity band due southwest of Vortex-c circulation, while the Vortex-c circulation transferred the vorticity outward, forming a vorticity wing evidently (Figs.1b-d). In the period from t=120 to 210 min, the circulations of Vortex-c and -d joined and the two vortices merged into a larger scale vortex. The inner-region vorticity mainly came from the circulation of Vortex-c. There existed two spiral vorticity bands in the outer region of the merged vortex, with its northerly band vorticity from the transferred Vortex-c's vorticity and the southerly band from the elongation of the Vortex-d circulation (Figs.1e-h).

Whereafter, the evolution of Vortex-e and -f can be seen from Fig.1. From t=0 to 90 min, Vortex-e and -f mutually rotated anticlockwise. When t=30 min, the exterior circulations of the two vortices approached but kept unattached (Fig.1b). At t=60 min, the vortices circulation deformed into a triangular shape evidently with their exterior circulation being joined (Fig.1c), which is a common phenomenon in the two vortices merging process. When t=90 min, the circulations of Vortex-e and -f both elongated (Fig.1d). In the next 120 minutes, the two vortices merged into one in the course of mutual rotation. Obviously, the inner-region vorticity of the merged vortex accumulated from that of the two vortices, with the two spiral vorticity bands in the outer region from the elongation of the vortices' circulation (Figs.1f-h).

Among the above three pairs of vortices, the scale of Vortex-a and -c is larger than that of Vortex-b and -d. The merging process of the two pairs of vortices is same, which means that the circulation of Vortex-b (or -d) is absorbed by Vortex-a (or -c) and elongates to form a spiral band of the merged vortex outer side. Another kind of merging process is that the two vortices near in scale played equivalent role for the final vortex formation, such as Vortex-e and -f merging. All the above results are coincident with those of Shen (2006). When t=210 min, the initial 12 vortices reduced to 9 through the process of two vortices merging (Fig.1h).

3.2 *Interactions of triple vortices under the condition of 9 vortices co-existing environment*

After 210 min of binary vortices interaction, there appeared three larger scale vortices (Fig.1h). Whereafter, the vortices, referred as Vortex-A, -B, and -C, rotated anticlockwise surrounded their geometrical center (Fig.2a). At t=6 h, a vorticity band was formed by the interactions of the four vortices located to the east of Vortex-a at t=210 min, with Vortex-F situated the westward to the band and Vortex-G the eastward (Fig.2a).

At t=12 h, Vortex-A, -B, and -C co-rotated around their geometrical center. Synchronously, the circulation of Vortex-E (or Vortex-G) was absorbed by that of Vortex-A (or Vortex-B), while the circulation of Vortex-F elongated to be a spiral band of Vortex-C (Fig.2b).

When t=18 h, the outer vorticity of Vortex-A and -B joined, which indicated the two vortices would be merged (Fig.2c).

Three hours later, Vortex-A, -B, and -C kept on co-rotating and their outer circulations connected together (Fig.2d).

In the period of 24-27 h, the circulation of Vortex-C stretched out to become a spiral band due south of Vortex-B, and the distance between Vortex-A and -B reduced with the elongating of Vortex-A circulation (Figs.2e-f).

At t=30 h, the circulation of Vortex-A became a spiral band to the west of Vortex-B (Fig.2g).

When t=33 h, a typhoon-like α-scale vortex was organized. The circulation of Vortex-C, which located

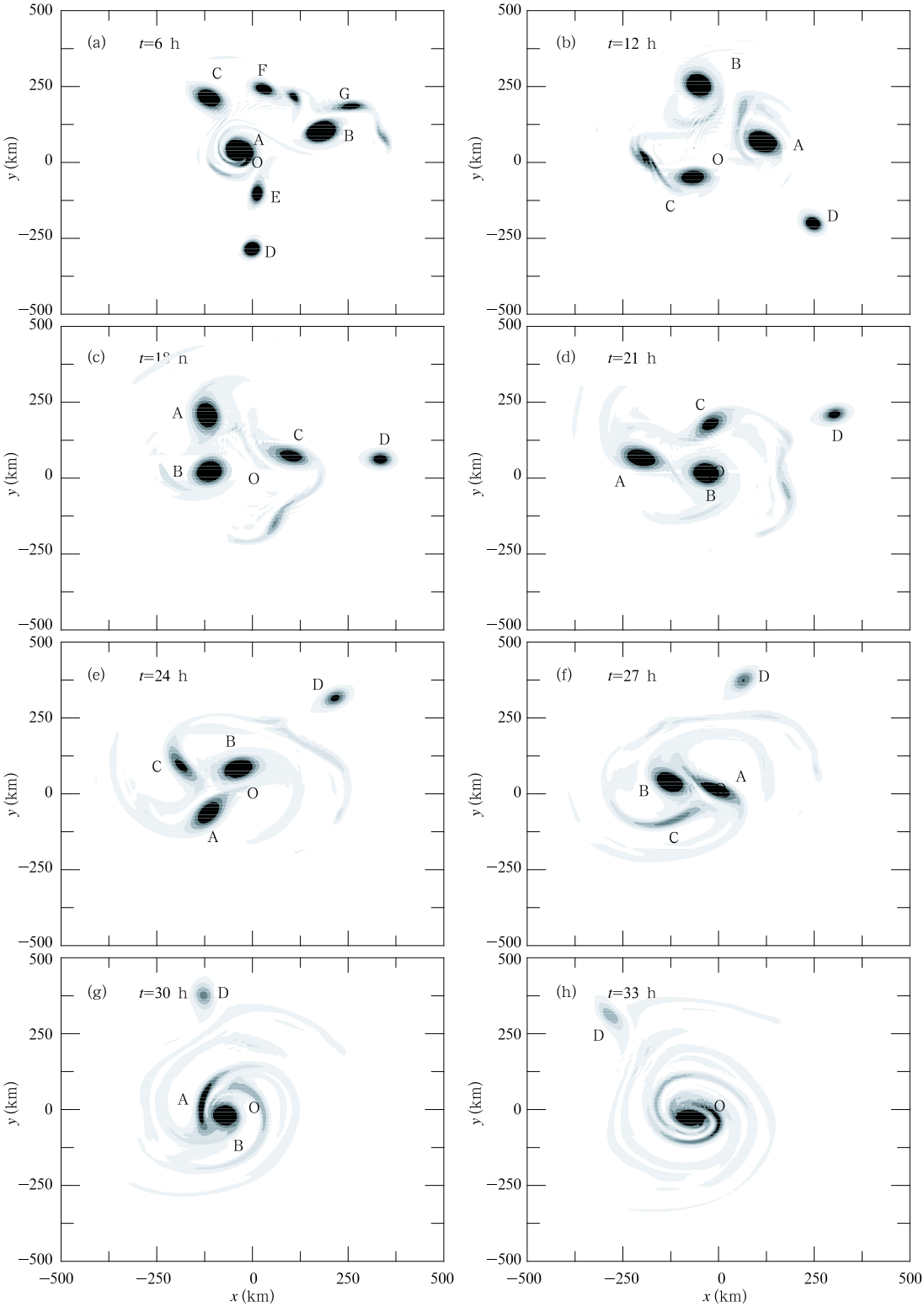

Fig.2. As in Fig.1, but for the period of 6-33 h. (a) t=6 h, (b) t=12 h, (c) t=18 h, (d) t=21 h, (e) t=24 h, (f) t=27 h, (g) t=30 h, and (h) t=33 h.

outside of the group of Vortex-A, -B, and -C, became one vorticity dump outside the merged vortex (Fig.2h). Thus, a larger scale vortex came into being through the self-organization process of the initial 12 scattered vortices.

3.3 *Analysis on the horizontal boundary effects on vortices self-organization process*

In the frame of self-organization dynamics, the effects of horizontal boundary can be ignored. In Experiment A, it is necessary to study the boundary effects for the reason that the circulation of Vortex-D was only 120 km away from the north boundary (Fig.2f). As such, the computational domain of Experiment B was expanded from 1000 km×1000 km to 1400 km×1400 km by extending 200 km in every direction, with the radii same as those of Experiment A. Figure 3 illustrated the vorticity temporal evolution of Experiment B.

By analyzing the results of the Experiments A and B (Figs.2 and 3), we can arrive at the conclusion that both self-organization processes are resemble, especially the evolution courses of Vortex-D in Experiments A and B (Figs.2g-h and Figs.3g-h). The results indicate that the initial vorticity field given by Eq.(1) was a high nonlinear system and that the change of size of the computational domain has no evident influence on the self-organization process. Hence, the outcome of Experiment A was convincing.

3.4 *Diverse initial vortex profiles effects on the self-organization process*

As discussed above, the largest initial vortex profiles in Experiments A and C were given, by 13 and 26 grid point values, respectively. The former is a coarse while the later is a fine description.

In this section, we will explore the influence of two types of vortex profile descriptions on the self-organization process. The vorticity field temporal change in Experiment C is shown in Fig.4.

In comparison with the vorticity field evolution shown in Figs.2 and 4, there are two resemblances as follows:

First, after integrating 6 h, the 12 vortices scattered in the initial field in two experiments reduced to 9 through the interaction of two close vortices circulation. And the distributions of 9 vortices in the two tests were similar (Figs.2a and 4a).

Second, ignoring Vortex-D, the 12 vortices in both tests first reduced to 9, subsequently became 3, then 2 vortices, and finally a larger scale vortex came into being through self-organization (Figs.2a-h and Figs. 4a-h).

The diversity of the results between the two tests indicates the influence of the precision of initial vortex profiles description on the self-organization process. Firstly, the mutual rotation speeds were not identical, such as in the period from 6 to 24 h, Vortex-B rotated about 390 degrees in Experiment A (Figs.2a-e) but 330 degrees in Experiment C (Figs.4a-d). Moreover, the speed of Vortex-D rotated around the group of the vortices in Experiment A was slower than that in Experiment C. Secondly, the vortices merging speed in Experiment A was faster than that in Experiment C. Finally, the inner-region vorticity were mainly from the circulation of Vortex-B in Experiment A (Figs.2e-h), while in Experiment C from the dump of the circulations of Vortex-A and -B (Figs.4f-h).

3.5 *Characteristics of enstrophy and eddy circulation*

The total kinetic energy and enstrophy, the analytical solutions, are conservation for the non-dissipation nonlinear system given by Eq.(1). In order to restrain the calculational instability caused by nonlinear, smoothing method was applied which suggested that weak dissipation was considered. In such a case, an important character of the 2-D quasi-geostrophic flow is selective dissipation. That is to say that the total kinetic energy decays slowly while the enstrophy does quickly. The temporal evolutions of the relative total kinetic energy, referred as R_e, and the relative enstrophy, referred as R_v, are illustrated in Figs.5a and b for the Experiment A. Here, we defined $R_e(t) = E(t)/E(0)$ and $R_v(t) = E_v(t)/E_v(0)$, where E and E_v denoted total kinetic energy and enstrophy, respectively.

It was well known that relative vorticity (referred as ξ, hereafter) denotes the rotation property of the tiny air mass and microcosmic movement of the eddy

flow. And that, the circulation, referred as Γ, illustrates the whole vortex rotation property and the macroscopical characteristic. The relative circulations of the largest vortex in the computation domain were

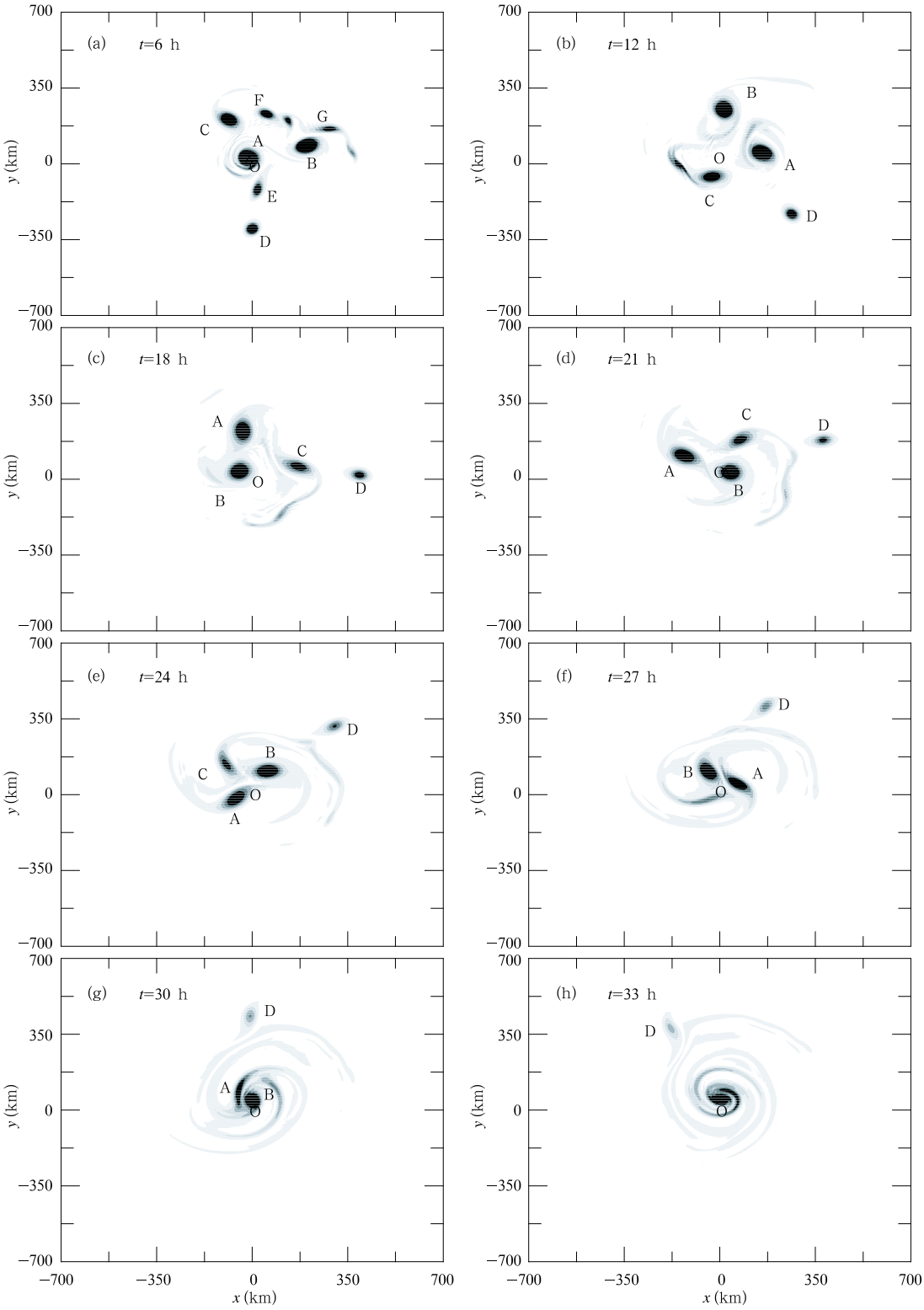

Fig.3. As in Fig.2, but for Experiment B.

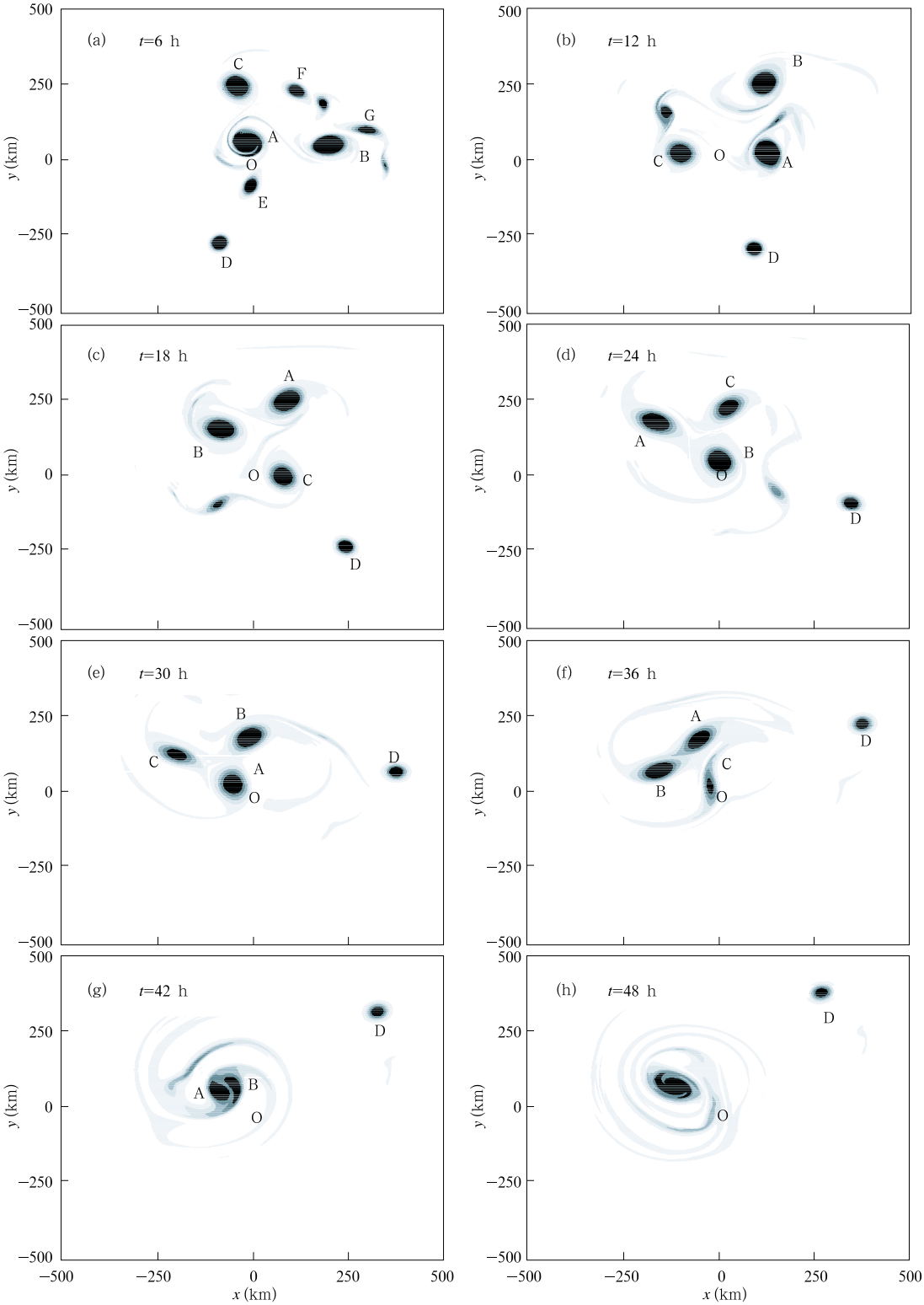

Fig.4. Temporal evolution of the relative vorticity field in Experiment C in the period of 6-48 h. (a) t=6 h, (b) t=12 h, (c) t=18 h, (d) t=24 h, (e) t=30 h, (f) t=36 h, (g) t=42 h, and (h) t=48 h; the shadings are the same as in Fig.2.

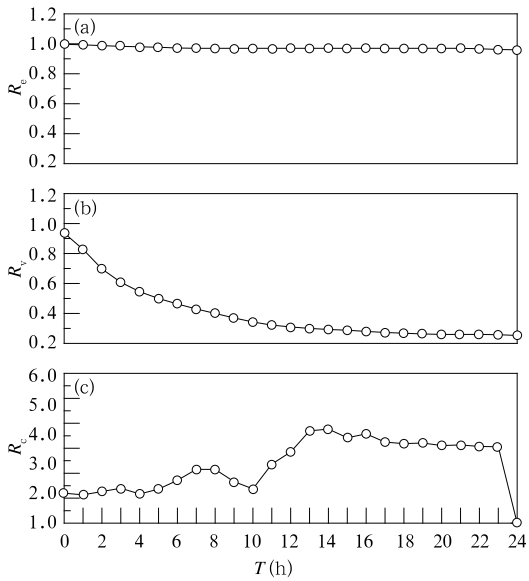

Fig.5. Temporal evolution of total relative energy R_e (a) and enstrophy R_v (b), and relative circulation R_c of the largest vortex (c) in Experiment A.

calculated every 3 h, referred as R_c, which was defined as $R_c = \Gamma(t)/\Gamma(0)$. Figure 5c shows the R_c temporal change.

It can be concluded from Fig.5 that the numerical solution singularity of the 2-D quasi-geostrophic flow self-organization process was that the total kinetic energy decayed slowly and the enstrophy did quickly with the largest vortex circulation increasing rapidly.

4. Results and discussions

In real atmosphere, observational facts of binary vortex merging have been found. For instance, the 9th and 10th typhoons of 1970 first moved westward and then merged into a larger one on the sea east of Taiwan Island before moving westward. The eyes of both typhoons still existed in the merged typhoon circulation and landfalled respectively on the central and southern areas of Fujian, causing difficulty in forecasting (Chen and Ding, 1979). Another good case was the development of Typhoon Oliver (Simpson et al., 1997).

Meanwhile, the observational facts of vortex merging are not just limited over the West Pacific Ocean. According to the nephogram analysis by Akiyama (1982), the synoptic, meso-α, -β, and -γ scale weather systems co-existed in the Meiyu front. Ding (1991) claimed that the meso-α scale weather system can be maintained by the merging of the meso-β scale systems.

Observational facts of vortex merging are not just limited to binary vortex interaction, but also include multi-vortex interactions. Up to now, as the most representative multi-vortex merging case was studied by Ma et al. (1997, see Fig.3 in their references), the merged cloud picture is used as the cover of the monograph meso-scale atmospheric dynamics proposed by Zhang (1999).

At present, remarkable progress in binary vortex merging dynamics has been made, but little has been done in the area of multi-vortex merging dynamics. Some work has been done in the study of the initial 8 vortices reduced to 5 through merging process with barotropic primitive equation model, but the vortices further evolution has not been carried out (Luo et al., 2002).

On the basis of the enhanced infrared satellite cloud picture (see Fig.3a) in the paper of Ma et al. (1997), 12 meso-β and -γ scale cloud clusters were identified. The vorticity distributions of the 12 vortices the same as the cloud cluster scattered in the picture were given in the same domain as the initial vorticity field for numerical study. The most valuable conclusion in the paper was that the self-organization process was a step-by-step merging course, namely the two adjacent vortecis first merged, then formed a triple vortex flow pattern, and finally organized into a meso-α scale vortex. Without diabatic forcing in the numerical simulation, the way the final vortex formed from the initial 12 vortices is attributed to self-organization process.

As the exploration in this paper was carried out in the frame of vortex self-organization dynamics, the results were obtained with idealization model. Whereas, as the multi-vortex merging process involves diverse physical mechanisms, further discussion will be carried out in our future papers.

Acknowledgements. We are deeply indebted to Professor Gao Shouting for his valuable help.

REFERENCES

Akiyama, T., 1990: Large, synoptic and mesoscale variations of the Baiu front during July 1982. Part III: Space time scale and structure of frontal disturbances. *J. Meteor. Soc. Japan*, **68**, 705-727.

Chen Lianshou and Ding Yihui, 1979: *A Panorama of Northwestern Pacific Typhoon*. Science Press, Beijing, 262-324. (in Chinese)

Chen Y., and M. K. Yau, 2001: Spiral bands in a simulated hurricane. Part I: Vortex Rossby wave verification. *J. Atmos. Sci.*, **58**, 2128-2145.

Ding Yihui, 1993: *The Research of Severe Heavy Rainfall Storm of Jianghuai River Valley in 1991*. China Meteorological Press, Beijing, 1-255. (in Chinese)

Luo Zhexian, Xu Xiangde, and Chen Lianshou, 2002: A preliminary study of the merge process of vorticity lumps. *Scientia Atmospherica Sinica*, **26**, 807-816. (in Chinese)

Ma Yu, Wang Xu, and Tao Zuyu, 1997: A survey of meso-scale convective systems and their temporal and spatial characteristics over China. *Progress in Natural Science*, **7**(6), 701-706. (in Chinese)

Shen Wu, Zhou Jialing, Ma Jingxian, Chen Lianshou, and Luo Zhexian, 2006: A study on interaction of non-asymmetric binary vortices. *Acta Meteorologica Sinica*, **64**(4), 453-463. (in Chinese)

Simpson, S. E. et al., 1997: Mesoscale interactions in tropical cyclogenesis. *Mon. Wea. Rev.*, **125**, 2643-2661.

Xie An, Xiao Wenjun, and Chen Shoujun, 1980: Energy budget of sub-synoptic scale disturbance during Meiyu period. *Acta Meteorologica Sinica*, **38**, 351-359. (in Chinese)

Xu Yamei and Gao Kun, 2002: Simulation and analysis of meso-β vortex over middle reaches of the Yangtze River on 22 July 1998. *Acta Meteorologica Sinica*, **60**, 85-95. (in Chinese)

Zhang Yuling, 1999: *Mesoscale Atmospheric Dynamics*. China Meteorological Press, Beijing, 1-313. (in Chinese)

Zheng Xinjiang, Tao Shiyan, Luo Jingyu, et al., 2001: Characteristics of meso-β scale cloud cluster in torrential rain process in Wuhan during 21-22 July 1998. *Acta Meteorologica Sinica*, **59**, 625-631. (in Chinese)